Int J Adv Manuf Technol (2008) 36:535–546
DOI 10.1007/s00170-006-0858-y

ORIGINAL ARTICLE

# NC data generation for 6-axis machine tools to produce a helical drill

**Jung-Fa Hsieh**

Received: 31 July 2006 / Accepted: 23 October 2006 / Published online: 29 November 2006


**Abstract** This study presents a design methodology for grinding a specific helical drill on a CNC 6-axis grinding machine. The proposed methodology comprises three steps: (1) deriving a mathematical model of the helical drill, (2) establishing the ability matrix of the multi-axis grinding machine according to Denavit-Hartenberg (D-H) notation, and (3) constructing configuration matrices to express the required grinding wheel positions and orientations while machining the flute and flank surfaces of the drill. The NC data for the motion values of each axis are obtained by equating the corresponding elements of the CNC ability matrix and the configuration matrices of the grinding wheel. To verify the proposed methodology, a designed helical drill is machined on a 6-axis CNC tool-grinding machine. The methodology presented in this study integrates the drill design and manufacturing activities, thereby making possible the implementation of a more flexible, automatic, cost efficient and controllable design and production process.

**Keywords** Helical drill · Denavit-Hartenberg (D-H) notation · Grinding

**Nomenclature**

| | |
|---|---|
| $(xyz)_0$ | coordinate frame $(xyz)_0$ built in drill |
| $(xyz)_t$ | coordinate frame $(xyz)_t$ built in grinding wheel |
| $(xyz)_c$ | coordinate frame $(xyz)_c$ built in helical grinder mechanism |
| ${}^0A_t$ | configuration matrix of grinding wheel frame $(xyz)_t$ with respect to drill frame $(xyz)_0$ |
| ${}^tq$ | generating curve of grinding wheel |
| ${}^tn$ | unit normal vector of grinding wheel |
| $r_{flute,i}$ | ith drill flute surface |
| $n_{flute,i}$ | unit outward normal vector of ith drill flute surface |
| $R_{flank,i}$ | ith drill flank surface |
| $\eta$ | required spindle rotation angle |
| $A$, $B$, $C$, $X$, $Y$, $Z$ | desired NC data for six axes of grinding machine |

J.-F. Hsieh (✉)
Department of Mechanical Engineering, Far East University, Hsin-Shih, Tainan 744, Taiwan
e-mail: seznof@cc.fec.edu.tw

## 1 Introduction

Micro-drills usually have a high length-to-diameter ratio (less than 0.5 mm in diameter and the aspect ratio is larger than 10), and are therefore suitable for producing deep holes. However, due to the small physical size of these drills, conventional point geometries, such as conical [1], spiral [2], cylindrical [3], multi-facet [4], etc. cannot be reproduced. Lin [5] proposed a mathematical model for the helical drill point and investigated the particular characteristics of this type of drill. It was shown that helical drill points provide a superior cutting performance in drilling operations, particularly in micro-hole drilling. However, the mathematical model proposed for grinding the helical drill could not be directly applied to machining on a multi-axis machine tool. Hsieh [6] also developed a helical point mathematical model based on the relationship between the helical drill point geometry and the grinding parameters.

The current study extends the mathematical model presented in [6] to grind a specific helical drill using a multi-axis CNC machine tool. The proposed design

methodology comprises three steps: (1) deriving a mathematical model for the helical drill, (2) constructing the ability matrix of the multi-axis CNC machine tool, and (3) establishing configuration matrices to express the required grinding wheel positions and orientations while grinding the flute and flank surfaces of the drill. To validate the proposed methodology, a specific helical drill is ground in accordance with the developed algorithm on a 6-axis CNC tool-grinding machine tool.

In this paper, the point vector $a_x i + a_y j + a_z k$ is written as a column matrix ${}^j a = [\, a_x \quad a_y \quad a_z \quad 1 \,]^T$, where the pre-superscript "j" of the leading symbol, ${}^j a$, indicates that the vector is defined with respect to the coordinate frame $(xyz)_j$. Given a point ${}^j a$, its transformation, ${}^k a$, is represented by the matrix product ${}^k a = {}^k A_j {}^j a$, where ${}^k A_j$ is a 4×4 matrix defining the position and orientation (referred to hereafter as the "configuration") of the frame $(xyz)_j$ with respect to a second frame $(xyz)_k$. The same notation rules are also applied to the unit directional vector, i.e. ${}^j n = [\, n_x \;\; n_y \;\; n_z \; 0 \,]^T$. Note that for reasons of simplicity, the pre-superscript "0" is omitted if a vector is referred to the drill frame $(xyz)_0$.

## 2 Drill design

This section of the paper reviews the helical drill design proposed in [6]. An important feature of any grinding wheel is the unit normal vector, ${}^t n$, along the working surface, ${}^t r$. The working surface of a helicoid grinding wheel can be obtained from its generating curve, ${}^t q = [\, h_i \quad 0 \quad f(h_i) \quad 1 \,]^T$ (where parameter $h_i$ varies over a specified range), in the $x_t$-$z_t$ plane rotation as it advances along the symmetrical $z_t$ axis (see Fig. 1). Consequently, the working surface of the tool, ${}^t r$, and its unit normal, ${}^t n$, with respect to the tool frame, $(xyz)_t$, can be expressed as:

$$ {}^t r = [\, h_i C v_i \quad h_i S v_i \quad f(h_i) + k_0 v_i \quad 1 \,]^T \tag{1} $$

$$ {}^t n = [\, n_x \quad n_y \quad n_z \quad 0 \,]^T = \frac{\partial {}^t r}{\partial h_i} \times \frac{\partial {}^t r}{\partial v_i} \Bigg/ \left| \frac{\partial {}^t r}{\partial h_i} \times \frac{\partial {}^t r}{\partial v_i} \right| = \frac{1}{\sqrt{k_0^2 + h_i^2 \left[ 1 + f'(h_i)^2 \right]}} [\, k_0 S v_i - h_i f'(h_i) C v_i \quad -h_i f'(h_i) S v_i - k_0 C v_i \quad h_i \quad 0 \,]^T \tag{2} $$

where C and S denote cosine and sine, respectively, and $k_0 = H/2\pi$, where $H$ is the pitch of the helix.

Although these equations relate to a helicoid grinding wheel, they can also be used to define an arbitrary revolution shape if $k_0$ is set to zero and its generating curve is given by $q^t = [\, x(h) \quad 0 \quad z(h) \quad 1 \,]^T$.

The geometry of the helical groove depends not only on the tool shape, but also on the machine setting parameters. Applying conjugate surface theory to determine the ith drill flute (Fig. 2), the following matrix can be obtained to describe the motion of the grinding wheel frame, $(xyz)_t$, relative to the drill frame, $(xyz)_0$:

$$ {}^0 A_{t,i} = Rot(x, 180^0) Trans(0, 0, a_z) Rot(z, \theta_i = \Omega t + 180^0 (i-1)) Trans(a_x, 0, 0) Rot(x, \lambda) Rot(y, \alpha) = \begin{bmatrix} C\theta_i C\alpha - S\theta_i S\lambda S\alpha & -S\theta_i C\lambda & C\theta_i S\alpha + S\theta_i S\lambda C\alpha & -a_x C\theta_i \\ -S\theta_i C\alpha - C\theta_i S\lambda S\alpha & -C\theta_i C\lambda & -S\theta_i S\alpha + C\theta_i S\lambda C\alpha & -a_x S\theta_i \\ C\lambda S\alpha & -S\lambda & -C\lambda C\alpha & -\alpha_z \\ 0 & 0 & 0 & 1 \end{bmatrix} \tag{3} $$

where parameters α and λ define the tool orientation required to generate the desired flute shape and the value of $180^0(i-1)$ gives the initial angular position of the tool required to produce the 1st and 2nd flutes. During machining, the grinding wheel rotates with an angular velocity Ω and advances simultaneously along the z- and x-axes of the drill frame $(xyz)_0$, with its position on the two axes defined by the displacement vectors $a_z = k_3 \Omega t$ and $a_x = a_{x0} + k_1 \Omega t$, respectively. Since the ith drill flute is generated in accordance with the principles of conjugate surface theory, the conjugate points and the complete flute profile can be determined from:

$$ n_i^T \frac{d(r_i)}{dt} = \left( {}^0 A_{t,i} \, {}^t r \right)^T \frac{d\left( {}^0 A_{t,i} \, {}^t r \right)}{dt} = 0 \tag{4} $$

where $r_i$ and $n_i$ are the flute surface equation and the unit outward normal with respect to frame $(xyz)_0$, respectively.

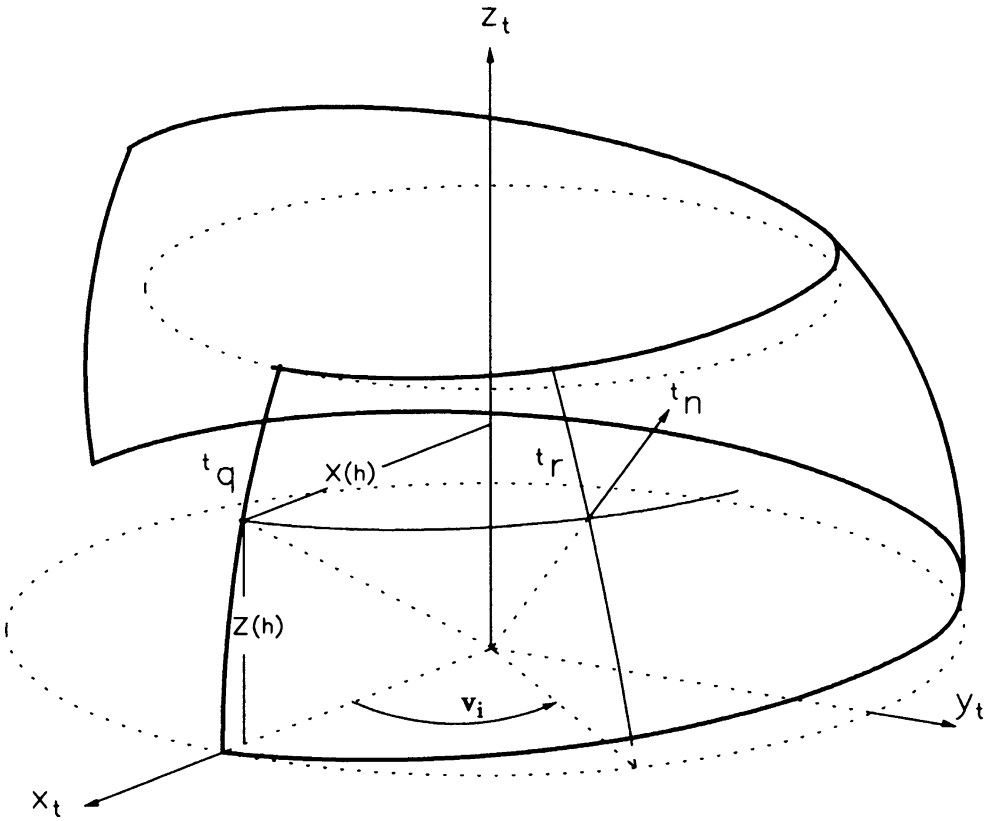


**Fig. 1** Generating curve and its unit outward normal vector [6]

At the conjugate point, the parameters $h$ and $v$ (denoted as $\overline{h}$ and $\overline{v}$, respectively) are related by:

$$\begin{aligned}
&-\left\{\left[x\left(\overline{h}\right)x'\left(\overline{h}\right)+z\left(\overline{h}\right)z'\left(\overline{h}\right)\right]S\lambda-z'\left(\overline{h}\right)\left(a_xS\lambda S\alpha+k_1C\alpha-k_3C\lambda S\alpha\right)\right\}C\overline{v}\\
&-\left\{\left[x\left(\overline{h}\right)x'\left(\overline{h}\right)+z\left(\overline{h}\right)z'\left(\overline{h}\right)\right]C\lambda S\alpha+z'\left(\overline{h}\right)\left(a_xC\lambda+k_3S\lambda\right)\right\}S\overline{v}\\
&-x'\left(\overline{h}\right)\left(a_xS\lambda C\alpha-k_1S\alpha-k_3C\lambda C\alpha\right)=0
\end{aligned} \tag{5}$$

The i[th] flute surface, $r_{flute,i}$, is obtained by substituting Eq. (5) into Eq. (1), and then transforming ${}^{t}r$ to frame $(xyz)_o$ via the transformation $r_{flute,i} = {}^{0}A_{t,i}\,{}^{t}r$, i.e.

$$\begin{aligned}
r_{flute,i} &= \left[\, r_{ix} \quad r_{iy} \quad r_{iz} \quad 1 \,\right]^T\\
&= \begin{bmatrix}
x\left(\overline{h}\right)\left(C\theta_iC\alpha-S\theta_iS\lambda S\alpha\right)C\overline{v}-x\left(\overline{h}\right)S\theta_iC\lambda S\overline{v}+z\left(\overline{h}\right)\left(C\theta_iS\alpha+S\theta_iS\lambda C\alpha\right)+a_xC\theta_i\\
-x\left(\overline{h}\right)\left(S\theta_iC\alpha+C\theta_iS\lambda S\alpha\right)C\overline{v}-x\left(\overline{h}\right)C\theta_iC\lambda S\overline{v}+z\left(\overline{h}\right)\left(-S\theta_iS\alpha+C\theta_iS\lambda C\alpha\right)-a_xS\theta_i\\
x\left(\overline{h}\right)C\lambda S\alpha C\overline{v}-x\left(\overline{h}\right)S\lambda S\overline{v}-z\left(\overline{h}\right)C\lambda C\alpha-k_3\Omega t\\
1
\end{bmatrix}
\end{aligned} \tag{6}$$

To obtain an expression for the ith flank surface, it is first necessary to derive the helicoid working surface of the form-grinding tool. In generating the ith flank surface, the relative configuration of the drill frame, $(xyz)_0$, with respect

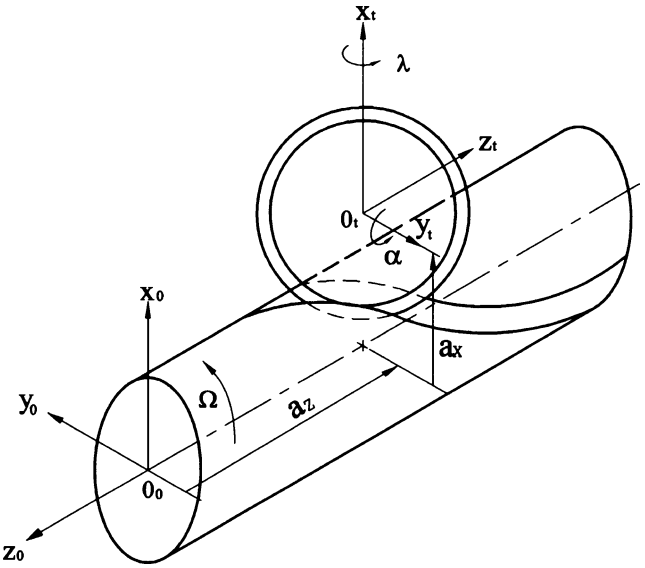


**Fig. 2** Cutting helical groove of helical drill [6]

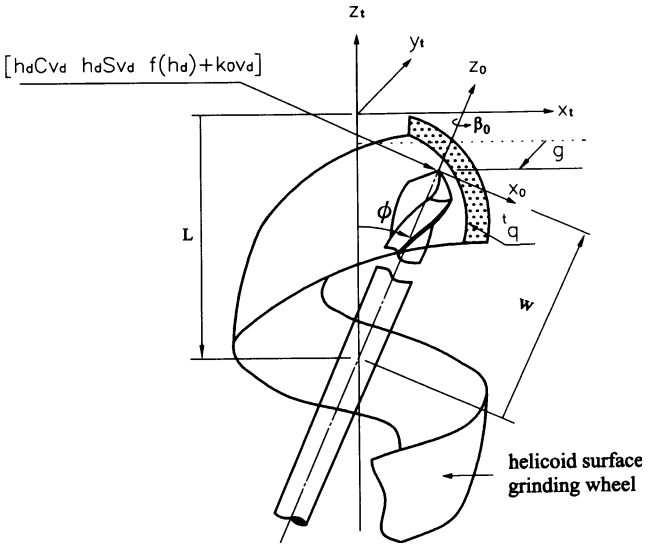


**Fig. 3** Grinding of drill flank surfaces using form_grinding tool [6]

to the tool frame, $(xyz)_t$, can be obtained by the following movements (Fig. 3):

$$
\begin{aligned}
{}^{t}A_0 &= Trans(0,0,-L)Rot(y,\psi)Trans(0,0,w)Trans(0,-g,0)Rot\left(z,\beta_i=\beta_0+180^0(i-1)\right)\\
&= \begin{bmatrix} C\psi C\beta_i & -C\psi S\beta_i & S\psi & wS\psi \\ S\beta_i & C\beta_i & 0 & -g \\ -S\psi C\beta_i & S\psi S\beta_i & C\psi & wC\psi - L \\ 0 & 0 & 0 & 1 \end{bmatrix}
\end{aligned} \tag{7}
$$

If the precise center of the flank surfaces is to lie at the origin of the drill frame, $(xyz)_0$, the fourth column of Eq. (7) must coincide with a point (denoted as $[h_dCv_d \quad h_dSv_d \quad f(h_d)+k_0v_d 1]^T$) on the working surface. As a result, two constraints exist between the parameters $v_d$, $h_d$, $g$, $L$, and $w$, namely:

$$Tan(v_d) = \frac{-g}{wS\psi} \tag{8}$$

$$L = wC\psi - f\left(\sqrt{w^2S^2\psi + g^2}\right) - k_0v_d \tag{9}$$

Finally, the ith flank surface, as expressed in the drill frame $(xyz)_0$, can be obtained by transforming the grinding tool working surface given in Eq. (1) to frame $(xyz)_0$, i.e.

$$
\begin{aligned}
R_{flank,i} &= {}^0A_t\,{}^tr\\
&= \begin{bmatrix} R_{ix} \\ R_{iy} \\ R_{iz} \\ 1 \end{bmatrix} = \begin{bmatrix} h_i[C\beta_iC\psi C\nu_i + S\beta_iS\nu_i] - [f(h_i)+k_0\nu_i+L]C\beta_iS\psi + gS\beta_i \\ h_i[-S\beta_iC\psi C\nu_i + C\beta_iS\nu_i] + [f(h_i)+k_0\nu_i+L]S\beta_iS\psi + gC\beta_i \\ h_iS\psi C\nu_i + [f(h_i)+k_0\nu_i+L]C\psi - w \\ 1 \end{bmatrix}
\end{aligned} \tag{10}
$$

Figure 4 presents the transverse section of a simulated helical drill at $r_{iz}$=0 (the core radius is 0.913). In this case, it is assumed that machining was performed using a bevel-type grinding wheel (see Fig. 5) with the generating curve derived in Appendix A and the following grinding parameters: $\alpha$=$10^0$, $\lambda$=$38^0$, $R$=6, $k_1 = 1.599/4\pi$, $k_3 = 65/2\pi$, and $a_{x0}$=49.8 (note that the length units used here (and hereafter) are mm). Figure 6 presents the front-end view of a simulated helical drill having the flute shapes shown in the cross-section of Fig. 4 machined using a form-grinding tool for which the generating curve is the line segment ${}^tq = [h_i \quad 0 \quad (38-h_i)/\tan(30^0)1]^T$. In this case, the grinding parameters are: $\psi$=$29^0$, $g$=8.205, $w$=87.065, $L$=152.919, $k_0$=11.937 and $\beta_0$=$3^0$.

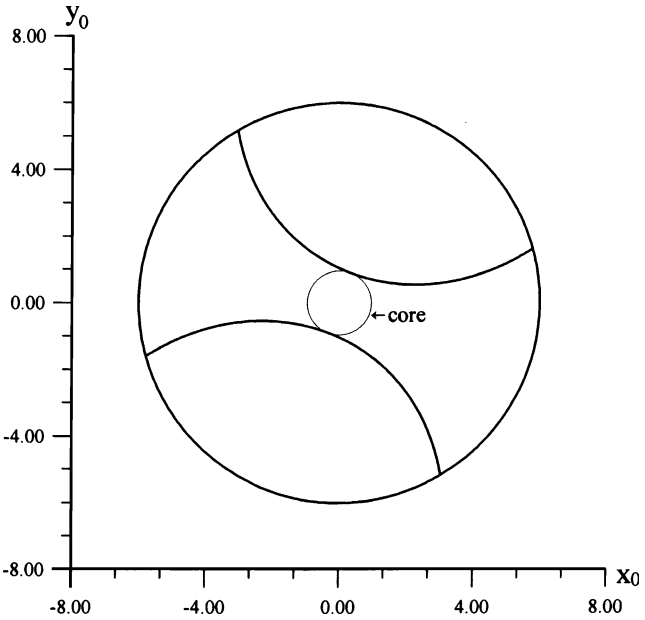


**Fig. 4** Transverse section of helical drill at $r_{iz}$=0

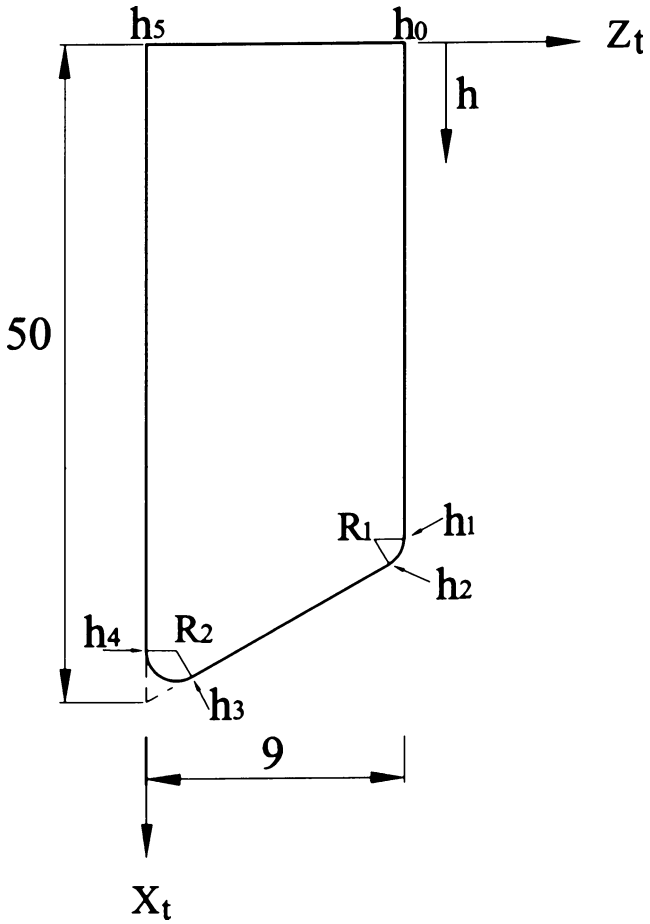


**Fig. 5** Generating curve of bevel–type grinding wheel

## 3 Ability matrix of tool-grinding machine

The grinding of helical drills is a complicated task that depends strongly type of tool-grinding machine employed. To determine the NC data to grind the helical drill, it is necessary establishing the ability matrix of the tool-grinding machine. This paper considers the case of an Ewag 6-axis CNC tool-grinding machine (see Fig. 7). Table 1 presents the various link parameters of this CNC machine according to Denavit-Hartenberg (D-H) notation.

The relative position and orientation of the spindle frame $(xyz)_{\underline{6}}$ with respect to the frame $(xyz)_{\underline{0}}$ can be expressed as:

$$
{}^{\underline{0}}A_{\underline{6}} = {}^{\underline{0}}A_{\underline{1}}{}^{\underline{1}}A_{\underline{2}}{}^{\underline{2}}A_{\underline{3}}{}^{\underline{3}}A_{\underline{4}}{}^{\underline{4}}A_{\underline{5}}{}^{\underline{5}}A_{\underline{6}}
$$

$$
= \begin{bmatrix}
C\underline{\theta}_1 S\underline{\theta}_2 S\underline{\theta}_6 - S\underline{\theta}_1 C\underline{\theta}_6 & C\underline{\theta}_1 C\underline{\theta}_2 & -C\underline{\theta}_1 S\underline{\theta}_2 C\underline{\theta}_6 - S\underline{\theta}_1 S\underline{\theta}_6 & -\underline{a}_6 S\underline{\theta}_1 C\underline{\theta}_6 + \underline{a}_6 C\underline{\theta}_1 S\underline{\theta}_2 S\underline{\theta}_6 + \underline{b}_5 C\underline{\theta}_1 C\underline{\theta}_2 - \underline{b}_4 C\underline{\theta}_1 S\underline{\theta}_2 + \underline{b}_3 S\underline{\theta}_1 + \underline{a}_1 C\underline{\theta}_1 \\
S\underline{\theta}_1 S\underline{\theta}_2 S\underline{\theta}_6 + C\underline{\theta}_1 C\underline{\theta}_6 & S\underline{\theta}_1 C\underline{\theta}_2 & C\underline{\theta}_1 S\underline{\theta}_6 - S\underline{\theta}_1 S\underline{\theta}_6 C\underline{\theta}_6 & \underline{a}_6 C\underline{\theta}_1 C\underline{\theta}_6 + \underline{a}_6 S\underline{\theta}_1 S\underline{\theta}_2 S\underline{\theta}_6 + \underline{b}_5 S\underline{\theta}_1 C\underline{\theta}_2 - \underline{b}_4 S\underline{\theta}_1 S\underline{\theta}_2 - \underline{b}_3 C\underline{\theta}_1 + \underline{a}_1 S\underline{\theta}_1 \\
C\underline{\theta}_2 S\underline{\theta}_6 & -S\underline{\theta}_2 & -C\underline{\theta}_2 C\underline{\theta}_6 & \underline{a}_6 C\underline{\theta}_2 S\underline{\theta}_6 - \underline{b}_5 S\underline{\theta}_2 - \underline{b}_4 C\underline{\theta}_2 + \underline{b}_1 \\
0 & 0 & 0 & 1
\end{bmatrix} \tag{11}
$$

where:

$$
{}^{\underline{i-1}}A_{\underline{i}} = \begin{bmatrix}
C\underline{\theta}_i & -S\underline{\theta}_i C\underline{\alpha}_i & S\underline{\theta}_i S\underline{\alpha}_i & \underline{a}_i C\underline{\theta}_i \\
S\underline{\theta}_i & C\underline{\theta}_i C\underline{\alpha}_i & -C\underline{\theta}_i S\underline{\alpha}_i & \underline{a}_i S\underline{\theta}_i \\
0 & S\underline{\alpha}_i & C\underline{\alpha}_i & \underline{b}_i \\
0 & 0 & 0 & 1
\end{bmatrix}
$$

Once the drill blank has been arbitrarily clamped in the clamping head, the position and orientation of the drill frame, $(xyz)_0$, with respect to the frame $(xyz)_{\underline{0}}$ are given by:

$$
{}^{0}A_{\underline{0}} = \begin{bmatrix}
1 & 0 & 0 & 0 \\
0 & 1 & 0 & 0 \\
0 & 0 & 1 & 0 \\
0 & 0 & 0 & 1
\end{bmatrix} \tag{12}
$$

From Fig. 8, it can be seen that the configuration matrix (relative orientation and position) of the tool frame, $(xyz)_t$,

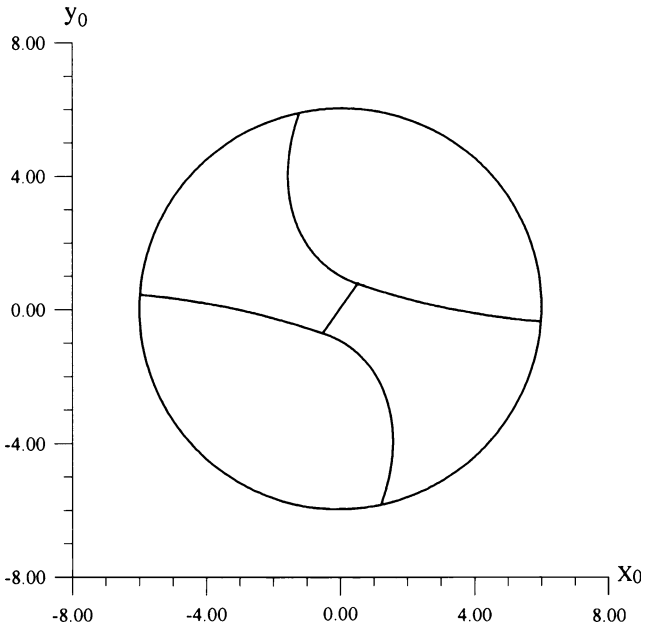


**Fig. 6** Front–end view of flanks and major cutting edges of helical drill

with respect to the spindle frame, $(xyz)_{\underline{6}}$, can be expressed as:

$$
{}^{\underline{6}}A_t = Rot(z,180^0)Rot(y,90^0)Trans(0,0,\underline{d})Rot(z,\eta)
= \begin{bmatrix} 0 & 0 & 1 & \underline{d} \\ -S\eta & -C\eta & 0 & 0 \\ -C\eta & S\eta & 0 & 0 \\ 0 & 0 & 0 & 1 \end{bmatrix} \tag{13}
$$

where $\underline{d}$ is the offset between the origins of frames $(xyz)_{\underline{6}}$ and $(xyz)_t$, respectively, and $\eta$ is the required spindle rotation. The configuration matrix of the grinding wheel frame, $(xyz)_t$, with respect to the drill frame, $(xyz)_0$, can be obtained as:

$$
{}^0A_t = {}^0A_{\underline{0}}A_{\underline{6}}{}^{\underline{6}}A_t
= \begin{bmatrix} {}^0I_{tx} & {}^0J_{tx} & {}^0K_{tx} & {}^0P_{tx} \\ {}^0I_{ty} & {}^0J_{ty} & {}^0K_{ty} & {}^0P_{ty} \\ {}^0I_{tz} & {}^0J_{tz} & {}^0K_{tz} & {}^0P_{tz} \\ 0 & 0 & 0 & 1 \end{bmatrix} \tag{14}
$$

Equation (14) is the ability matrix, ${}^0A_t$, of the tool-grinding machine. The elements of this matrix are given in Appendix B.

**Table 1** Kinematic parameters of tool-grinding machine

| Pa./Link | 1 | 2 | 3 | 4 | 5 | 6 |
|---|---|---|---|---|---|---|
| $b_i$ | $\underline{b}_1$ | 0 | $\underline{b}_3$ | $\underline{b}_4$ | $\underline{b}_5$ | 0 |
| $\theta_i$ | $\underline{\theta}_1$ | $\underline{\theta}_2$ | 0 | $-90^0$ | 0 | $\underline{\theta}_6$ |
| $a_i$ | $\underline{a}_1$ | 0 | 0 | 0 | 0 | $\underline{a}_6$ |
| $\alpha_i$ | $-90^0$ | $180^0$ | $-90^0$ | $-90^0$ | $0^0$ | $-90^0$ |

## 4 NC data for flank grinding

In the grinding process shown in Fig. 3, the drill is fixed as the grinder moves. Due to the limitations of current manufacturing technologies, helicoid surface grinding wheels do not actually exist. Hence, when using a CNC grinding machine to form the helical flank, a simple generating curve of ${}^tq$ is generally used. Under these machining conditions, the grinding wheel can be considered as a dresser and the drill blank as a clamped tool. If the dresser (grinding wheel) can successfully dress the shape of

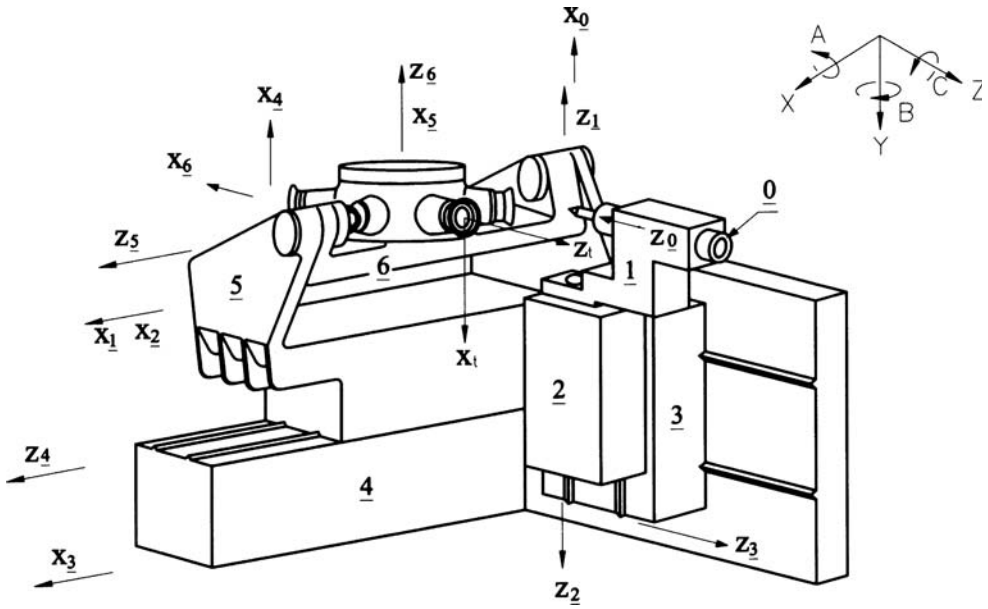


**Fig. 7** Ewag CNC 6–axis tool–grinding machine

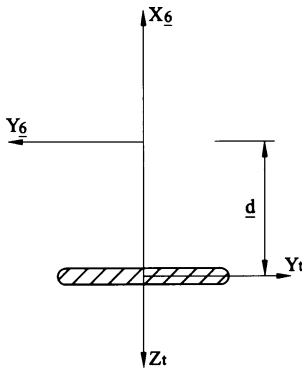


**Fig. 8** Tool setting on tool–grinding machine

the helicoid grinding wheel, then it can also grind the desired flank shape.

To produce the helicoid surface shown in Fig. 3, it is first necessary to establish the coordinate system assignments and to define the grinding parameters. The initial position of the origin, $o_c$, located at the intersection of the grinding wheel spindle axis and the helical axis, $z_c$, is assigned in the $(xyz)_c$ coordinate system, where the frame $(xyz)_c$ is considered to be a helical mechanism. In other words, during flank surface grinding, the frame $(xyz)_c$ rotates with respect to the $z_c$ axis and advances along the $z_c$ axis in accordance with the helix pitch, $H$. From Fig. 9, it can be shown that the position and orientation of the grinding wheel, $(xyz)_t$, with respect to the frame$(xyz)_c$ are given by:

$$
\begin{aligned}
{}^{c}A_t &= Rot(z,-\Gamma)Trans(0,0,-k_0\Gamma)Rot(y,\xi)Trans(0,0,\rho)Rot(z,-\nu)\\
&= \begin{bmatrix} C\Gamma C\xi C\nu - S\Gamma S\nu & C\Gamma C\xi S\nu + S\Gamma C\nu & C\Gamma S\xi & \rho C\Gamma S\xi \\ -S\Gamma C\xi C\nu - C\Gamma C\nu & -S\Gamma C\xi S\nu + C\Gamma C\nu & -S\Gamma S\xi & -\rho S\Gamma S\xi \\ -S\xi C\nu & -S\xi S\nu & C\xi & \rho C\xi - k_0\Gamma \\ 0 & 0 & 0 & 1 \end{bmatrix}
\end{aligned} \tag{15}
$$

where $\nu$ is the polar angle of the working generating curve ${}^{t}q$ of the grinding wheel and parameters $\xi$ and $\rho$ define the relative positions and orientations, respectively, of frames $(xyz)_c$ and $(xyz)_t$.

From Fig. 8, it can be seen that a generating curve ${}^{c}q$ of the helicoid surface can be obtained by using a grinding wheel with the same generating curve. The desired flank shape can then be ground by positioning the drill blank on the face of the grinding wheel (see Fig. 10).

The position and orientation of the frame $(xyz)_c$ with respect to the frame $(xyz)_0$ (compare $(xyz)_c$ with the frame $(xyz)_t$ in Fig. 3) are given by:

$$
\begin{aligned}
{}^{0}A_c &= Rot(z,-\beta_i)Trans(0,g,0)Trans(0,0,-w+\varepsilon)Rot(y,-\psi)Trans(0,0,L)\\
&= \begin{bmatrix} C\psi C\beta_i & S\beta_i & -S\psi C\beta_i & -LS\psi C\beta_i + gS\beta_i \\ -C\psi S\beta_i & C\beta_i & S\psi S\beta_i & LS\psi S\beta_i + gC\beta_i \\ S\psi & 0 & C\psi & LC\psi - (w-\varepsilon) \\ 0 & 0 & 0 & 1 \end{bmatrix}
\end{aligned} \tag{16}
$$

where $\beta_i = \beta_0 + 180^0(i-1)$ and the parameter $\varepsilon$ is the machining allowance during the grinding process. Note that over cutting will occur if $\varepsilon<0$.

The product of the matrices given in Eq. (15) and Eq. (16) gives the configuration matrix of the grinding wheel frame, $(xyz)_t$, with respect to the drill frame, $(xyz)_0$, i.e.

$$
{}^{0}A_t = {}^{0}A_c\,{}^{c}A_t \tag{17}
$$

The link variables of the current 6-axis CNC machine can be solved and the spindle rotation angle, $\eta$, obtained by equating the corresponding elements of Eqs. (14) and (17). However, solving this matrix equation is difficult, and hence both sides of the equation are multiplied by $\left({}^{5}_{\underline{5}}A_{\underline{6}}\,{}^{6}A_t\right)^{-1}$ to give:

$$
{}^{0}A_{\underline{5}} = \begin{bmatrix} -S\underline{\theta}_1 & C\underline{\theta}_1 S\underline{\theta}_2 & C\underline{\theta}_1 C\underline{\theta}_2 & \underline{b}_5 C\underline{\theta}_1 C\underline{\theta}_2 - \underline{b}_4 C\underline{\theta}_1 S\underline{\theta}_2 + \underline{b}_3 S\underline{\theta}_1 + \underline{a}_1 C\underline{\theta}_1 \\ C\underline{\theta}_1 & S\underline{\theta}_1 S\underline{\theta}_2 & S\underline{\theta}_1 C\underline{\theta}_2 & \underline{b}_5 S\underline{\theta}_1 C\underline{\theta}_2 - \underline{b}_4 S\underline{\theta}_1 S\underline{\theta}_2 - \underline{b}_3 C\underline{\theta}_1 + \underline{a}_1 S\underline{\theta}_1 \\ 0 & C\underline{\theta}_2 & -S\underline{\theta}_2 & \underline{b}_5 S\underline{\theta}_2 - \underline{b}_4 C\underline{\theta}_2 + \underline{b}_1 \\ 0 & 0 & 0 & 1 \end{bmatrix} = \begin{bmatrix} I'_x & J'_x & K'_x & P'_x \\ I'_y & J'_y & K'_y & P'_y \\ I'_z & J'_z & K'_z & P'_z \\ 0 & 0 & 0 & 1 \end{bmatrix} \tag{18}
$$

Note that the elements of this equation are given in Appendix C.

From element (3,1) of Eq. (18), the spindle rotation angle, $\eta$ ($0^0 \le \eta \le 180^0$), can be solved by:

$$\begin{aligned} I_z' = &-(S\psi C\Gamma S\xi + C\psi C\xi)C\underline{\theta}_6 - [S\psi(C\Gamma C\xi Cv - S\Gamma Sv) - C\psi S\xi Cv]C\eta S\underline{\theta}_6 \\ &+ [S\psi(C\Gamma C\xi Sv + S\Gamma Cv) - C\psi S\xi Sv]S\eta S\underline{\theta}_6 = 0 \end{aligned} \tag{19}$$

Equating the third and fourth columns of Eq. (18), the link variables of the machine are obtained as:

$$\underline{\theta}_1 = \tan^{-1}\left(-I_x'\Big/I_y'\right) \tag{20}$$

$$\underline{\theta}_2 = \tan^{-1}\left(-K_z'\Big/J_z'\right) \tag{21}$$

$$\begin{aligned} \underline{b}_3 = &[\underline{a}_6 - \underline{d} + \rho - gS\Gamma S\xi + (h - k_0\Gamma)C\xi]C\underline{\theta}_6 \\ &+ [g(-S\Gamma C\xi CvC\eta - C\Gamma SvC\eta + S\Gamma C\xi SvS\eta - C\Gamma CvS\eta) + (h - k_0\Gamma)S\xi(SvS\eta - CvC\eta)]S\underline{\theta}_6 \end{aligned} \tag{22}$$

$$\begin{aligned} \underline{b}_4 = &[(\underline{a}_6 - \underline{d} + \rho + (h - k_0\Gamma)C\xi - gS\Gamma S\xi)S\underline{\theta}_6 + [(h - k_0\Gamma)S\xi CvC\eta - (h - k_0\Gamma)S\xi SvS\eta - gS\Gamma C\xi SvS\eta + gS\Gamma C\xi CvC\eta + gC\Gamma CvS\eta + gC\Gamma SvC\eta]C\underline{\theta}_6 \\ &+ \underline{a}_1(S\psi C\Gamma C\xi Cv - S\psi S\Gamma Sv - C\psi S\xi Cv)S\eta + \underline{a}_1(S\psi C\Gamma C\xi Sv + S\psi S\Gamma Cv - C\psi S\xi Sv)C\eta \\ &- (w - \varepsilon + \underline{b}_1)(S\psi C\Gamma S\xi + C\psi C\xi)S\underline{\theta}_6 + (w - \varepsilon + \underline{b}_1)(S\psi C\Gamma S\xi Cv - S\psi S\Gamma Sv - C\psi S\xi Cv) \\ &C\eta C\underline{\theta}_6 - (w - \varepsilon + \underline{b}_1)(S\psi C\Gamma C\xi Sv + S\psi S\Gamma Cv - C\psi S\xi Sv)S\eta C\underline{\theta}_6 \end{aligned} \tag{23}$$

$$\begin{aligned} \underline{b}_5 = &\underline{a}_1(S\psi C\Gamma S\xi + C\psi C\xi)S\underline{\theta}_6 - \underline{a}_1[(S\psi C\Gamma C\xi Cv - S\psi S\Gamma Sv - C\psi S\xi Cv)C\eta - (S\psi C\Gamma C\xi Sv + S\psi S\Gamma Cv - C\psi S\xi Sv)S\eta]C\underline{\theta}_6 \\ &+ (w - \varepsilon + \underline{b}_1)[(S\psi C\Gamma C\xi Cv - S\psi S\Gamma Sv - C\psi S\xi Cv)S\eta + (S\psi C\Gamma C\xi Sv + S\psi S\Gamma Cv - C\psi S\xi Sv)C\eta] \\ &+ (h - k_0\Gamma)S\xi(SvC\eta + CvS\eta) - gS\Gamma C\xi(SvC\eta + CvS\eta) - gC\Gamma(CvC\eta - SvS\eta) \end{aligned} \tag{24}$$

In Fig. 7, when $\underline{\theta}_1 = 270^0$, $\underline{\theta}_2 = 0^0$ and $\underline{\theta}_6 = 90^0$, and the origin of frame $(xyz)_t$ coincides with the origin of the drill frame, $(xyz)_0$, the configuration of frame $(xyz)_t$ with respect to $(xyz)_0$ is given by:

$${}^0A_t = \begin{bmatrix} -C\eta & S\eta & 0 & 0 \\ S\eta & C\eta & 0 & 0 \\ 0 & 0 & -1 & 0 \\ 0 & 0 & 0 & 1 \end{bmatrix} = \begin{bmatrix} -C\eta & S\eta & 0 & \underline{b}_3 \\ S\eta & C\eta & 0 & -\underline{a}_1 - \underline{b}_5 \\ 0 & 0 & -1 & -\underline{d} + \underline{a}_6 - \underline{b}_4 + \underline{b}_1 \\ 0 & 0 & 0 & 1 \end{bmatrix} \tag{25}$$

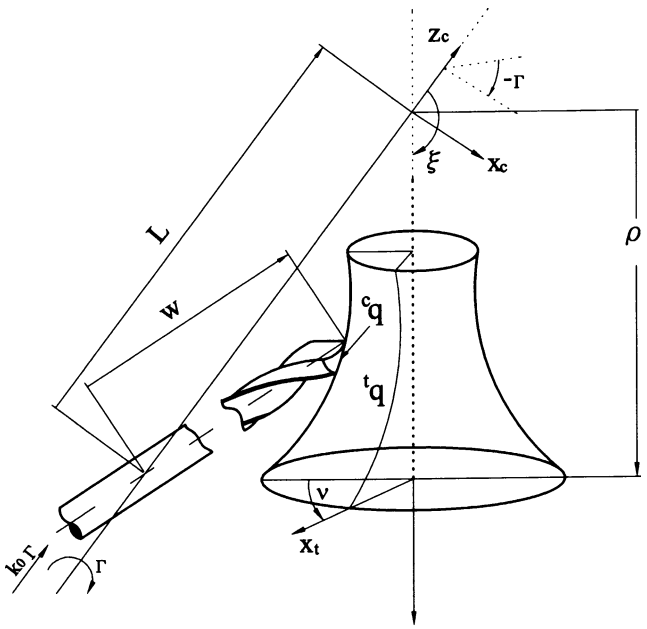


**Fig. 9** Coordinate system assignments and grinding parameter definitions for helical grinding method

By equating the corresponding elements of Eq. (25), the following expressions for the joint variables can be obtained:

$$\underline{\theta}_{10} = 270^0 \tag{26}$$

$$\underline{\theta}_{20} = 0^0 \tag{27}$$

$$\underline{b}_{30} = 0^0 \tag{28}$$

$$\underline{b}_{40} = \underline{a}_6 + \underline{b}_1 - \underline{d} \tag{29}$$

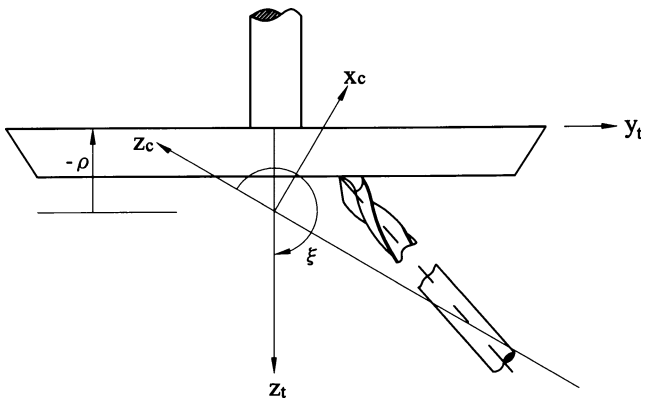


**Fig. 10** Grinding flanks using bevel grinder

$$\underline{b}_{50} = -\underline{a}_1 \tag{30}$$

$$\underline{\theta}_{60} = 90^0 \tag{31}$$

The NC data equations of the A, B, C, X, Y and Z axes required to produce the flank surfaces can then be obtained from the corresponding differences between the joint variables $\underline{\theta}_1$, $\underline{\theta}_2$, $\underline{b}_3$, $\underline{b}_4$, $\underline{b}_5$, $\underline{\theta}_6$ and $\underline{\theta}_{10}$, $\underline{\theta}_{20}$, $\underline{b}_{30}$, $\underline{b}_{40}$, $\underline{b}_{50}$, $\underline{\theta}_{60}$, respectively, i.e.

$$X = \underline{b}_5 - \underline{b}_{50} \tag{32}$$

$$Y = -(\underline{b}_3 - \underline{b}_{30}) \tag{33}$$

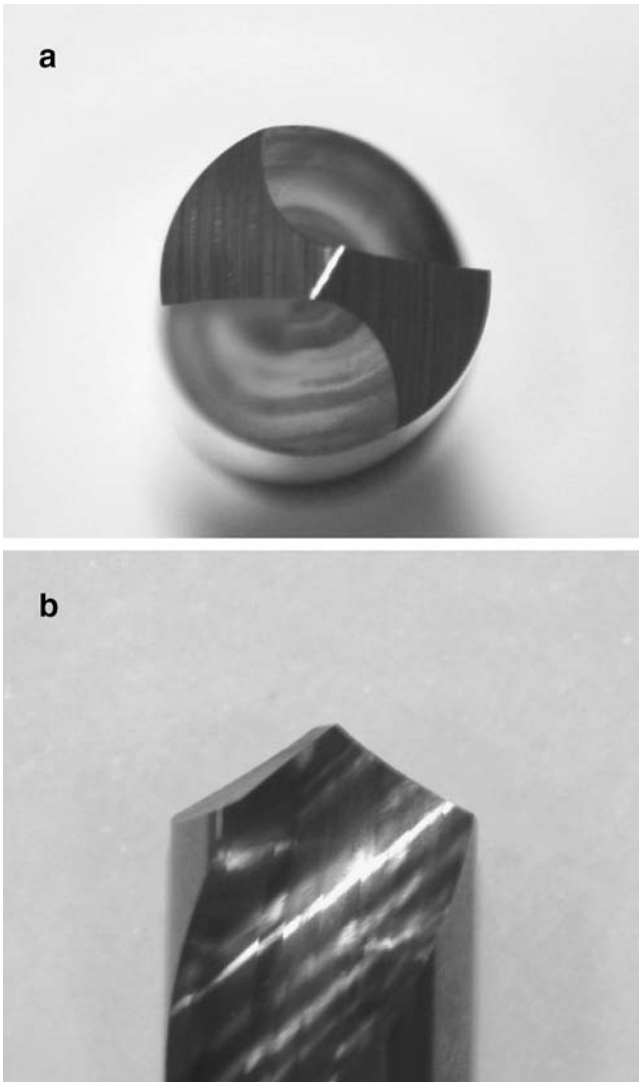


**Fig. 11** A helical drill

$$Z = -(\underline{b}_4 - \underline{b}_{40}) \tag{34}$$

$$A = \underline{\theta}_6 - \underline{\theta}_{60} \tag{35}$$

$$B = \underline{\theta}_2 - \underline{\theta}_{20} \tag{36}$$

$$C = \underline{\theta}_1 - \underline{\theta}_{10} \tag{37}$$

Equations (32)–(37) yield the NC code necessary to produce the drill flanks on the 6-axis Ewag CNC tool-grinding machine considered in this study. (Note that the methodology for obtaining the NC data required to grind the drill flutes is presented by Hsieh and Lin in [7]).

## 5 Implementation

To demonstrate the validity of the proposed methodology, the helical drill designed in Section 2 was ground on the 6-axis Ewag CNC tool-grinding machine using a bevel-type grinding wheel with the generating curve given in Eqs. (A1–A5) and the grinding parameters indicated in Section 2. It is noted that the flank grinding parameters in Fig. 10 were respectively set as $\xi$=240$^0$, $\rho$=–(9+30C30$^0$)% $\nu$=–90$^0$. Figure 11 presents drill points ground based on helical flank surface. When Figs. 6 and 11 are compared, it is clear that a satisfactory agreement phenomenon occurs between the simulated drill and the ground drill. Therefore, the ability of the proposed methodology to provide a satisfactory description of a helical drill is confirmed.

## 6 Conclusion

This paper has presented a methodology for obtaining the NC data required to grind a helical drill using a 6-axis CNC tool-grinding machine. In the proposed approach, homogenous transformation matrices are employed to develop the ability matrix of the tool-grinding machine and to determine the desired cutter locations. The NC data equations are then obtained by equating the corresponding elements of the ability matrix and the cutter location matrices. Applying the proposed modeling process, an illustrative example has been presented to validate the performance of the proposed methodology. The proposed approach integrates the design and manufacturing activities, thereby making possible a more flexible, automatic, and controllable production process.

**Acknowledgements** The author gratefully acknowledges the financial support provided by the National Science Council of Taiwan under grant NSC94-2212-E-269-015. Author is also obliged to Diku Diamond Enterprise Co. Ltd for providing technical assistance.

## Appendix A

$$0 \le h \le h_1 \begin{cases} x_t = h \\ z_t = 9. \end{cases} \tag{A1}$$

$$h_1 \le h \le h_2 \begin{cases} x_t = h_1 + R_1 S\left(\frac{h-h_1}{R_1}\right) \\ z_t = 9. - R_1 + R_1 C\left(\frac{h-h_1}{R_1}\right) \end{cases} \tag{A2}$$

$$h_2 \le h \le h_3 \begin{cases} x_t = h_1 + \frac{\sqrt{3}R_1}{2} + \frac{h-h_2}{2} \\ z_t = 9. - \frac{R_1}{2} - \frac{\sqrt{3}(h-h_2)}{2} \end{cases} \tag{A3}$$

$$h_3 \le h \le h_4 \begin{cases} x_t = h_1 + \frac{\sqrt{3}R_1}{2} + \frac{h_3-h_2}{2} + \frac{\sqrt{3}R_2}{2} C\left(\frac{h-h_3}{R_2}\right) + \frac{R_2}{2} S\left(\frac{h-h_3}{R_2}\right) - \frac{\sqrt{3}R_2}{2} \\ z_t = 9. - \frac{R_1}{2} - \frac{\sqrt{3}(h-h_2)}{2} + \frac{R_2}{2} C\left(\frac{h-h_3}{R_2}\right) - \frac{\sqrt{3}R_2}{2} S\left(\frac{h-h_3}{R_2}\right) - \frac{R_2}{2} \end{cases} \tag{A4}$$

$$h_4 \le h \le h_5 \begin{cases} x_t = h_5 - h \\ z_t = 0 \end{cases} \tag{A5}$$

where $h_1 = 50 - 3\sqrt{3} - R_1/\sqrt{3}$, $h_2 = h_1 + R_1\pi/3$, $h_3 = h_2 + (18 - R_1)/\sqrt{3}, h_4 = h_3 + 2\pi r R_2/3 h_5 = h_4 + 50 - \sqrt{3}R_2, R_1 = 0.1, R_2 = 1$

## Appendix B

$${}^0I_{tx} = -C\underline{\theta}_1 C\underline{\theta}_2 S\eta + (S\underline{\theta}_1 S\underline{\theta}_6 + C\underline{\theta}_1 S\underline{\theta}_2 C\underline{\theta}_6) C\eta \tag{B1}$$

$${}^0I_{ty} = -S\underline{\theta}_1 C\underline{\theta}_2 S\eta - (C\underline{\theta}_1 S\underline{\theta}_6 - S\underline{\theta}_1 S\underline{\theta}_2 C\underline{\theta}_6) C\eta \tag{B2}$$

$$^{0}I_{tz} = S\underline{\theta}_2 S\eta + C\underline{\theta}_2 C\underline{\theta}_6 C\eta \tag{B3}$$

$$^{0}J_{tx} = -C\underline{\theta}_1 C\underline{\theta}_2 C\eta - (S\underline{\theta}_1 S\underline{\theta}_6 + C\underline{\theta}_1 S\underline{\theta}_2 C\underline{\theta}_6)S\eta \tag{B4}$$

$$^{0}J_{ty} = -S\underline{\theta}_1 C\underline{\theta}_2 C\eta + (C\underline{\theta}_1 S\underline{\theta}_6 - S\underline{\theta}_1 S\underline{\theta}_2 C\underline{\theta}_6)S\eta \tag{B5}$$

$$^{0}J_{tz} = S\underline{\theta}_2 C\eta - C\underline{\theta}_2 C\underline{\theta}_6 S\eta \tag{B6}$$

$$^{0}K_{tx} = S\underline{\theta}_1 C\underline{\theta}_6 - C\underline{\theta}_1 S\underline{\theta}_2 S\underline{\theta}_6 \tag{B7}$$

$$^{0}K_{ty} = -C\underline{\theta}_1 C\underline{\theta}_6 - S\underline{\theta}_1 S\underline{\theta}_2 C\underline{\theta}_6 \tag{B8}$$

$$^{0}K_{tz} = -C\underline{\theta}_2 S\underline{\theta}_6 \tag{B9}$$

$$^{0}P_{tx} = (\underline{a}_6 - \underline{d})C\underline{\theta}_1 S\underline{\theta}_2 S\underline{\theta}_6 - (\underline{a}_6 - \underline{d})S\underline{\theta}_1 C\underline{\theta}_6 + \underline{b}_5 C\underline{\theta}_1 C\underline{\theta}_2 - \underline{b}_4 C\underline{\theta}_1 S\underline{\theta}_2 + \underline{b}_3 S\underline{\theta}_1 + \underline{a}_1 C\underline{\theta}_1 \tag{B10}$$

$$^{0}P_{ty} = (\underline{a}_6 - \underline{d})C\underline{\theta}_1 C\underline{\theta}_6 + (\underline{a}_6 - \underline{d})S\underline{\theta}_1 S\underline{\theta}_2 S\underline{\theta}_6 + \underline{b}_5 S\underline{\theta}_1 C\underline{\theta}_2 - \underline{b}_4 S\underline{\theta}_1 S\underline{\theta}_2 - \underline{b}_3 C\underline{\theta}_1 + \underline{a}_1 S\underline{\theta}_1 \tag{B11}$$

$$^{0}P_{tz} = (\underline{a}_6 - \underline{d})C\underline{\theta}_2 S\underline{\theta}_6 - \underline{b}_5 S\underline{\theta}_2 - \underline{b}_4 C\underline{\theta}_2 + \underline{b}_1 \tag{B12}$$

## Appendix C

$$I_x' = -(C\psi C\beta_i C\Gamma S\xi - S\beta_i S\Gamma S\xi - S\psi C\beta_i C\xi)C\underline{\theta}_6 - [C\psi C\beta_i - (C\Gamma C\xi C\nu - S\Gamma S\nu) - S\beta_i(S\Gamma C\xi C\nu + C\Gamma S\nu) + S\psi C\beta_i S\xi C\nu]C\eta S\underline{\theta}_6 + [C\psi C\beta_i(C\Gamma C\xi S\nu + S\Gamma C\nu) + S\beta_i(-S\Gamma C\xi S\nu + C\Gamma C\nu) + S\psi C\beta_i S\xi S\nu]S\eta S\underline{\theta}_6 \tag{C1}$$

$$I_y' = (C\psi S\beta_i C\Gamma S\xi + C\beta_i S\Gamma S\xi - S\psi S\beta_i C\xi)C\underline{\theta}_6 + [C\psi S\beta_i(C\Gamma C\xi C\nu - S\Gamma S\nu) + C\beta_i(S\Gamma C\xi C\nu + C\Gamma S\nu) + S\psi S\beta_i S\xi C\nu]C\eta S\underline{\theta}_6 - [C\psi S\beta_i(C\Gamma C\xi S\nu + S\Gamma C\nu) - C\beta_i(-S\Gamma C\xi S\nu + C\Gamma C\nu) + S\psi S\beta_i S\xi S\nu]S\eta S\underline{\theta}_6 \tag{C2}$$

$$I_z' = -(S\psi C\Gamma S\xi + C\psi C\xi)C\underline{\theta}_6 - [S\psi(C\Gamma C\xi C\nu - S\Gamma S\nu) - C\psi S\xi C\nu]C\eta S\underline{\theta}_6 + [S\psi(C\Gamma C\xi S\nu + S\Gamma C\nu) - C\psi S\xi S\nu]S\eta S\underline{\theta}_6 \tag{C3}$$

$$J_x' = -(C\psi C\beta_i C\Gamma S\xi - S\beta_i S\Gamma S\xi - S\psi C\beta_i C\xi)S\underline{\theta}_6 + [C\psi C\beta_i(C\Gamma C\xi C\nu - S\Gamma S\nu) - S\beta_i(S\Gamma C\xi C\nu + C\Gamma S\nu) + S\psi C\beta_i S\xi C\nu]C\eta C\underline{\theta}_6 - [C\psi C\beta_i(C\Gamma C\xi S\nu + S\Gamma C\nu) + S\beta_i(-S\Gamma C\xi S\nu + C\Gamma C\nu) + S\psi C\beta_i S\xi S\nu]S\eta C\underline{\theta}_6 \tag{C4}$$

$$J_y' = -(-C\psi S\beta_i C\Gamma S\xi - C\beta_i S\Gamma S\xi + S\psi S\beta_i C\xi) S\underline{\theta}_6 + [-C\psi S\beta_i (C\Gamma C\xi C\nu - S\Gamma S\nu) - C\beta_i (S\Gamma C\xi C\nu + C\Gamma S\nu) - S\psi S\beta_i S\xi C\nu] C\eta C\underline{\theta}_6 - [-C\psi S\beta_i (C\Gamma C\xi S\nu + S\Gamma C\nu) + C\beta_i (-S\Gamma C\xi S\nu + C\Gamma C\nu) - S\psi S\beta_i S\xi S\nu] S\eta C\underline{\theta}_6 \quad \text{(C5)}$$

$$J_z' = -(S\psi C\Gamma S\xi + C\psi C\xi) S\underline{\theta}_6 + [S\psi (C\Gamma C\xi C\nu - S\Gamma S\nu) - C\psi S\xi C\nu] C\eta S\underline{\theta}_6 - [S\psi (C\Gamma C\xi S\nu + S\Gamma C\nu) - C\psi S\xi S\nu] S\eta C\underline{\theta}_6 \quad \text{(C6)}$$

$$K_x' = -[C\psi C\beta_i (C\Gamma C\xi C\nu - S\Gamma S\nu) - S\beta_i (S\Gamma C\xi C\nu + C\Gamma S\nu) + S\psi C\beta_i S\xi C\nu] S\eta - [C\psi C\beta_i (C\Gamma C\xi S\nu + S\Gamma C\nu) + S\beta_i (-S\Gamma C\xi S\nu + C\Gamma C\nu) + S\psi C\beta_i S\xi S\nu] C\eta \quad \text{(C7)}$$

$$K_y' = [C\psi S\beta_i (C\Gamma C\xi C\nu - S\Gamma S\nu) + C\beta_i (S\Gamma C\xi C\nu + C\Gamma S\nu) + S\psi S\beta_i S\xi C\nu] S\eta + [C\psi S\beta_i (C\Gamma C\xi S\nu + S\Gamma C\nu) - C\beta_i (-S\Gamma C\xi S\nu + C\Gamma C\nu) + S\psi S\beta_i S\xi S\nu] C\eta \quad \text{(C8)}$$

$$K_z' = -[S\psi (C\Gamma C\xi C\nu + S\Gamma S\nu) - C\psi S\xi C\nu] S\eta - [S\psi (C\Gamma C\xi S\nu - S\Gamma C\nu) - C\psi S\xi S\nu] C\eta \quad \text{(C9)}$$

$$P_x' = (\underline{a}_6 - \underline{d})(C\psi C\beta_i C\Gamma S\xi - S\beta_i S\Gamma S\xi - S\psi C\beta_i C\xi) + C\psi C\beta_i \rho C\Gamma S\xi - S\beta_i \rho S\Gamma S\xi - S\psi C\beta_i (\rho C\xi - k_0\Gamma) - LC\beta_i S\psi + gS\beta_i \quad \text{(C10)}$$

$$P_y' = (\underline{a}_6 - \underline{d})(-C\psi S\beta_i C\Gamma S\xi - C\beta_i S\Gamma S\xi + S\psi S\beta_i C\xi) - C\psi S\beta_i \rho C\Gamma S\xi - C\beta_i \rho S\Gamma S\xi + S\psi S\beta_i (\rho C\xi - k_0\Gamma) + LS\beta_i S\psi + gC\beta_i \quad \text{(C11)}$$

$$P_z' = (\underline{a}_6 - \underline{d})(S\psi C\Gamma S\xi + C\psi C\xi) + S\psi \rho C\Gamma S\xi + C\psi (\rho C\xi - k_0\Gamma) + LC\psi - (w - \varepsilon) \quad \text{(C12)}$$

## References


1. Galloway DF (1957) Some Experiments on the influence of various factors on drill performance. Trans ASME 79:191–231
2. Ernst H, Haggerty WA (1958) The spiral point drill-a new concept in drill point geometry. Trans ASME 80:1059–10721
3. Fugelso MA (1983) Cylindrical flank twist drill point. ASME J Eng Ind 105:183–186
4. Wu SM, Shen JM (1983) Mathematical model for muti-facet Drills. ASME J Eng Ind 105:177–182
5. Lin C, Kang SM, Ehmann KF (1995) Helical micro-drill point design and grinding. ASME J Eng Ind 117(3):277–287
6. Hsieh JF (2005) Mathematical Model for Helical drill point. J Mach Tool Manuf 45:967–977
7. Hsieh JF, Lin PD (2003) Production of multifluted drills on six-axis CNC tool-grinding machine. Int J Mach Tool Manuf 43:1117–1127